Revision of the Dissociation Energies of Mercury Chalcogenides—Unusual Types of Mercury Bonding

Michael Filatov* and Dieter Cremer*[a]

Mercury chalcogenides HgE (E = O, S, Se, etc.) are described in the literature to possess rather stable bonds with bond dissociation energies between 53 and 30 kcal mol^{-1}, which is actually difficult to understand in view of the closed-shell electron configuration of the Hg atom in its ground state (…4f^{14}5d^{10}6s^2). Based on relativistically corrected many body perturbation theory and coupled-cluster theory [IORAmm/MP4, Feenberg-scaled IORAmm/MP4, IORAmm/CCSD(T)] in connection with IORAmm/B3LYP theory and a [17s14p9d5f]/aug-cc-pVTZ basis set, it is shown that the covalent HgE bond is rather weak (2–7 kcal mol^{-1}), the ground state of HgE is a triplet rather than a singlet state, and that the experimental bond dissociation energies have been obtained for dimers (or mixtures of monomers, dimers, and even trimers) Hg_2E_2 rather than true monomers. The dimers possess association energies of more than 100 kcal mol^{-1} due to electrostatic forces between the monomer units. The covalent bond between Hg and E is in so far peculiar as it requires a charge transfer from Hg to E (depending on the electronegativity of E) for the creation of a single bond, which is supported by electrostatic forces. However, σ bonding between Hg and E is reduced by strong lone pair–lone pair repulsion to a couple of kcal mol^{-1}. Since a triplet configuration possesses somewhat lower destabilizing lone pair energies, the triplet state is more stable. In the dimer, there is a Hg–Hg π bond of bond order 0.66 without any σ support. Weak covalent Hg–O interactions are supported by electrostatic bonding. The results for the mercury chalcogenides suggests that all experimental dissociation energies for group-12 chalcogenides have to be revised because of erroneous measurements.

1. Introduction

Mercury monoxide HgO is assumed to play an important role in the mercury depletion events in the atmosphere. It was suggested that gaseous elemental mercury can react in the troposphere with halogen oxides such as BrO to yield mercury monoxide which can be deposited on the surface.[1–4]

Whereas solid mercury monoxide (and other mercury chalcogenides) is well-known and well-characterized,[5] the information about gaseous HgO is controversial. Originally, gaseous HgO was tentatively identified by infrared spectroscopy in rare gas matrices under nonstationary vaporization conditions.[6] Later, mass spectrometric measurements suggested[7] a dissociation energy D_0 of 53 ± 8 kcal mol^{-1} for HgO, which implied that the reaction of gaseous elemental mercury with bromine oxide should be nearly thermoneutral [D_0(BrO) = 55.2 ± 0.4 kcal mol^{-1} as obtained from heats of formation at 0 K[8]]. However, recent high-level ab initio calculations predict for the dissociation energy D_e of HgO a 50 kcal mol^{-1} lower value of just 4 kcal mol^{-1}.[9,10] Such a weak bonding between mercury and oxygen in HgO implies that the reaction Hg + BrO → Br + HgO is strongly endothermic[10] and excludes a scenario in which mercury monoxide is responsible for the depletion of mercury in the atmosphere.[10]

Although the quantum-chemical investigations on mercury oxide[9,10] address an important issue of the atmospheric chemistry of mercury, little is revealed about the reason for such an enormous (ca. 50 kcal mol^{-1}) discrepancy between theory and experiment. Normally, the application of high-level theoretical methods such as coupled-cluster theory to diatomic molecules leads to dissociation energies (and other bond properties) well within the accuracy of measured properties ($\pm$1–2 kcal mol^{-1}).[11] However, if one excludes a drastic failure of theory, then there will only be the possibility that another mercury species instead of HgO was measured in the experiment. This of course would have serious implications for the understanding of the chemistry of mercury,[12,13] and even the chemistry of the other group-12 compounds, namely Zn and Cd:

1) Besides HgO, also HgS and HgSe were investigated and dissociation energies D_0 of 52 ± 5 and 35 ± 7 kcal mol^{-1},[7] respectively, were measured for these compounds. Any inconsistency between theory and experiment found for HgO should also apply to the other mercury chalcogenides HgE.
2) The bonding in HgO was so far considered as that of an ionic oxide in view of the large difference in the electronegativities χ(O) = 3.50 and χ(Hg) = 1.44.[5,13] However, a dissociation energy of just 4 kcal mol^{-1}[9,10] is more typical of a van der Waals complex than an ionic oxide. This contradiction requires a re-investigation of bonding in HgO and other mercury chalcogenides. The situation becomes even

[a] *Dr. M. Filatov, Prof. Dr. D. Cremer*
Department of Theoretical Chemistry, Göteborg University
Reutersgatan 2, 41320 Göteborg (Sweden)
Fax: (+46) 317-735-590
E-mail: filatov@theoc.gu.se
dieter.cremer@theoc.gu.se

 DOI: 10.1002/cphc.200301207

more complicated by the fact that the ground state of HgO and other HgE molecules is a triplet rather than a singlet as we will show in the following.

3) Any new observation for mercury compounds HgE is of direct relevance for gaseous chalcogenides ZnE and CdE because these compounds should possess similar bonding features and similar properties.
4) In view of the contradictory results for HgO it is not likely that this compound is involved in the mechanism of mercury depletion from the atmosphere. Does a clarification of the mercury oxide problem lead to a new mechanism of mercury oxidation in the atmosphere?

The mass spectrometric measurements for mercury oxide definitely identified a mercury oxygen compound.[7] The question is only whether HgO or a species $(HgO)_n$ with n = 2, 3… rather n = 1 was found because for all values of *n* the same charge/mass ratio will be found. For example, judging from the electronegativities of elemental mercury and oxygen, the gas-phase mercury monoxide should be a polar molecule with a large dipole moment. Dipole–dipole interactions between two HgO molecules should facilitate the formation of a dimeric species, which can be further stabilized by interactions between the charged mercury atoms. The existence of Hg–Hg bonded cationic species, such as Hg^{2+}, in the condensed phase is well-documented.[12,13] Accordingly, the potential existence of a dimeric species $(HgO)_2$ in the gas phase merits a careful investigation.

There is also the possibility that a O_2^{2-} unit is formed, which is then bridged by two Hg^+ ions. Diamond-shaped peroxides with electropositive substituents (Li or BeH)[14] or transition metal atoms[15,16] have been discussed in the literature. Therefore, we will also consider both isomeric forms of the mercury oxide dimer, which can be related by bond stretch isomerism.[15]

To the best of our knowledge, the stability of the HgO dimer or, more generally, of mercury chalcogenide dimers $(HgE)_2$ (E = O, S, Se) have not been studied so far in the literature. It is the primary objective of the present paper to carry out relativistically corrected high-level ab initio calculations for the monomeric HgE and dimeric $(HgE)_2$ (E = O, S, Se) species and to study their relative stabilities and bonding features. If the dimeric mercury chalcogenides happen to be considerably more stable than the monomeric species, the discrepancy between measured[7] and calculated dissociation energies for the monomeric species[9,10] can be explained as resulting from dimerization (or even polymerization) of monomeric species in the gas phase. This would be the basis for answering questions that emerge in connection with points 1) to 4) mentioned above.

2. Computational Methods

For the monomeric HgE (E = O, S, Se) species, many body Møller–Plesset (MP) perturbation theory[17] was used at second (MP2), third (MP3), and fourth order (MP4) where in the latter case all single (S), double (D), triple (T), and quadruple (Q) excitations were included thus yielding MP4(SDTQ) = MP4(full) results. The effect of T excitations was evaluated by comparing MP4(full) results with those of MP4(SDQ) calculations. For the purpose of including infinite order effects into the SD space, coupled-cluster theory[18] with all S and D excitations (CCSD)[19a] was used, which was extended by a perturbational treatment of T excitations to CCSD(T).[19b] In all ab initio calculations, the 4f, 5s, 5p, 5d, and 6s electrons of mercury were correlated together with the 2s, 2p electrons of O, the 3s, 3p electrons of S, and the 3s, 3p, 3d, 4s, 4p electrons of Se.

In the ab initio calculations, the geometry of the monomeric species was optimized numerically. The dimeric species $(HgE)_2$ (E = O, S, Se) were calculated only with the MP methods because the coupled-cluster calculations could not be performed due to limited computer resources. Only single-point calculations were possible for the dimers utilizing geometries obtained by density functional theory (DFT) calculations with the B3LYP hybrid density functional.[20,21] The B3LYP geometry optimizations employed analytic energy gradients and were performed for both monomeric and dimeric species. The natural bond orbital (NBO) analysis[22] was employed at the B3LYP level of theory to determine reliable atomic charges.

The singlet and the triplet states were calculated for all monomeric and dimeric species. The singlet states were calculated with the closed-shell spin-restricted formalism and the triplet states with the spin-unrestricted formalism.

The monomeric HgE and dimeric $(HgE)_2$ (E = O, S, Se) species are typified by electron clustering at the same center. These species belong to type B systems in the Cremer-He classification of electronic systems.[23] For these systems, the convergence of the MP series is nonmonotonous and it can be smoothened out substantially[24,25] with the help of Feenberg scaling.[26] Within the Feenberg extrapolation scheme,[24–26] the improved value of the correlation energy is obtained from individual orders of the MP*n* series using Equation (1),

$$\Delta E^{(4)}_{\lambda^{(3)}} = (1-\lambda^{(3)})E^{(2)}_{MP} + \lambda^{(3)}(1-\lambda^{(3)})^2 E^{(3)}_{MP} + (1-\lambda^{(3)})^3 E^{(4)}_{MP} \quad (1)$$

where the parameter $\lambda^{(3)}$ is defined in Equation (2).

$$\lambda^{(3)} = 1 - \frac{E^{(2)}_{MP}}{E^{(2)}_{MP} - E^{(3)}_{MP}} \quad (2)$$

Generally, the energies obtained from the Feenberg scaling procedure are more reliable than the corresponding MP4 energies and they can be compared in quality to coupled-cluster energies.[24,25] Therefore, Feenberg scaling was performed for all MP4 calculations of the monomeric and dimeric species.

A [17s14p9d5f] basis set was employed for mercury. The basis set was constructed from the uncontracted (19s14p10d5f) Hg basis set of Gropen[27] in the following way. In the original basis set, the most diffuse set of primitive d-type gaussian-type functions (GTFs) was removed to avoid linearity problems. One s-type, four p- and d-type, and three f-type sets of diffuse GTFs were added in a well tempered sequence using an exponent ratio of 2.5. Five s-type GTFs (#4 to #8 in the original basis) were contracted to two s-type basis functions according to a 3/2 pattern. The eight inner p-type

GTFs were contracted to three p-type basis functions using a 3/3/2 contraction pattern. Seven tight d-type sets of GTFs were contracted according to a 3/2/1/2 pattern and the four most tight f-type sets of GTFs were contracted to one set. The resulting [17s14p9d5f] basis set was combined with the augmented triple-zeta correlation consistent basis set (aug-cc-pVTZ) of Dunning.[28] All calculations employed cartesian GTFs.

The relativistic effects were included with the help of the infinite-order regular approximation with modified metric (IORAmm) method described in our earlier publications.[29,30] The energetical consequences of possible spin–orbit (SO) interactions were neglected in the quasi-relativistic IORAmm calculations. Since the present work deals with either closed-shell species or with open-shell species where unpaired electrons are located in the 6s orbital of mercury or in the valence p orbitals of the chalcogen atoms, this scalar-relativistic approximation is acceptable. The total energies obtained in the IORAmm calculations were corrected for the gauge-shift error as described in the previous publications.[29,30]

Table 1. *Optimized bond lengths, dissociation energies, harmonic vibrational frequencies, and dipole moments of singlet and triplet states of monomeric HgE (E = O, S, Se) species. All calculations employ the IORAmm quasirelativistic Hamiltonian.*

Molecule (State)	Parameter	B3LYP[a]	CCSD(T)[a]	MP2[a]	MP4[b]	$FE^{(4)}_{\lambda^{(3)}}$ [b,c]
HgO ($^1\Sigma^+$)	r_e [Å]	1.878	1.875	1.816		
	ω_e [cm^{-1}]	641	642	792		
	D_e [kcal mol^{-1}]	2.59	2.91	11.42	10.86	4.31
	μ [Debye]	4.97		5.55		
	q_{NBO} [e]	±0.903				
HgO ($^3\Pi$)	r_e [Å]	2.214	2.145	2.102		
	ω_e [cm^{-1}]	267	322	320		
	D_e [kcal mol^{-1}]	9.81	4.20	0.09	2.21	2.17
	μ [Debye]	2.38		2.05		
	q_{NBO} [e]	±0.413				
HgS ($^1\Sigma^+$)	r_e [Å]	2.265	2.253	2.209		
	ω_e [cm^{-1}]	341	363	377		
	D_e [kcal mol^{-1}]	6.74	6.28	10.03	9.58	7.19
	μ [Debye]	5.07		6.51		
	q_{NBO} [e]	±0.696				
HgS ($^3\Pi$)	r_e [Å]	2.580	2.535	2.580		
	ω_e [cm^{-1}]	173	183	98		
	D_e [kcal mol^{-1}]	8.68	6.10	3.24	5.17	4.76
	μ [Debye]	2.40		2.77		
	q_{NBO} [e]	±0.327				
HgSe ($^1\Sigma^+$)	r_e [Å]	2.393	2.374	2.327		
	ω_e [cm^{-1}]	217	264	244		
	D_e [kcal mol^{-1}]	1.60	1.77	4.81	4.72	1.57
	μ [Debye]	5.12		6.55		
	q_{NBO} [e]	±0.624				
HgSe ($^3\Pi$)	r_e [Å]	2.703	2.681	2.753		
	ω_e [cm^{-1}]	118	164	52		
	D_e [kcal mol^{-1}]	4.83	3.82	1.66	2.77	1.71
	μ [Debye]	2.58		2.85		
	q_{NBO} [e]	±0.282				

[a] Optimized with the respective method. [b] Calculated at the IORAmm/B3LYP geometry. [c] $\lambda^{(3)}$ Feenberg extrapolation energy obtained from the fourth-order IORAmm/MP energy.

The dissociation asymptote Hg $^1S + O\,^3P$ is used throughout this work as a reference regardless of the actual molecular spin state. The use of this asymptote (and not that of Hg $^1S + O\,^1D$ which would fit the singlet states but is 45.4 kcal mol^{-1} higher in energy[31]) is justified because, in the actual gas-phase systems, the spin–orbit coupling (neglected in the present calculations) would mix the states of different multiplicity. Although, for the equilibrium geometries, the first-order spin-orbit effects are expected to be small due to the reasons just described (which is also confirmed by the results of ref. [9]), the mixing of singlet and triplet molecular states is possible for dissociating molecules due to the presence of the heavy element Hg. Thus, the Hg $^1S + O\,^3P$ dissociation limit is chosen in order to obtain estimates of the dissociation energy close to the real situation in the gas phase.

All calculations were carried out with the help of the COLOGNE2003 suite of quantum-chemical programs.[32]

3. Results and Discussion

The results of calculations are summarized in Tables 1–4. Table 1 shows the spectroscopic parameters for the monomeric HgE (E = O, S, Se) species. The bond length, dissociation energy, and harmonic vibrational frequency of HgO in the singlet $^1\Sigma^+$ state obtained in the present work by the IORAmm/CCSD(T) calculations (r_e = 1.875 Å, ω_e = 642 cm^{-1}, D_e = 2.91 kcal mol^{-1}) are in reasonable agreement with the parameters obtained previously by Shepler and Peterson[9] in DK/CCSD(T) (DK: Douglas–Kroll; r_e = 1.912 Å, ω_e = 601 cm^{-1}, D_e = 2.69 kcal mol^{-1}) and relativistic effective core potentials (RECP)/CCSD(T) (r_e = 1.912 Å, ω_e = 599 cm^{-1}, D_e = 2.79 kcal mol^{-1}) calculations, which employed a sequence of correlation-consistent basis sets to extrapolate results to the basis set limit. This justifies the choice of the basis sets used in the present work. Note, that in the latter calculations[9] only the valence electrons, that is, the 5d and 6s of the Hg atom and the 2s and 2p of the O atom, were correlated, whereas our calculations correlate also the 4f, 5s, and 5p electrons of the Hg atom.

The results of the IORAmm/B3LYP geometry optimizations for the monomeric species are in excellent agreement with the IORAmm/CCSD(T) results (see Table 1). Thus, it can be anticipated that the use of IORAmm/B3LYP for the geometry optimization of dimers $(HgE)_2$ (E = O, S, Se) should be also acceptable. Note that the overall size of the basis set reaches as many as 464 contracted functions for $(HgSe)_2$, which renders the application of CCSD(T) impossible due to limited computational re-

sources. Even the full MP4 calculation of the triplet $(HgSe)_2$ cluster could not be finished due to prohibitive requirements for disk space.

Before we start a detailed discussion of the bonding patterns in the monomeric and dimeric mercury chalcogenides, a comment on the role of relativity for bonding is appropriate. Relativity results in a contraction of the 6s orbital and an increase in the first ionization potential of mercury. As it has been observed in previous calculations on HgO, this makes the Hg–O bond shorter and weaker.[9] A substantial (ca. 0.11 Å) shortening with a simultaneous weakening (ca. 20 kcal mol^{-1}) of the HgO bond is confirmed by a comparison of the nonrelativistic B3LYP results for the singlet $^1\Sigma^+$ ($r_e = 1.987$ Å, $D_e = 17.47$ kcal mol^{-1}) and the triplet $^3\Pi$ state ($r_e = 2.216$ Å, $D_e = 25.80$ kcal mol^{-1}) of mercury oxide with the results of the IORAmm/B3LYP calculations reported in Table 1. The relativistic decrements in the bond length and bond strength obtained by the IORAmm/B3LYP calculations coincide closely with those obtained by Shepler and Peterson[9] in the all-electron DK/CCSD(T) calculations. This confirms that relativity plays an important role for the mercury chalcogenides and without its inclusion the results of theoretical calculations may point in the wrong direction when considering the stability of monomeric and dimeric species. Therefore, we will discuss exclusively the results of the quasi-relativistic IORAmm calculations in the following.

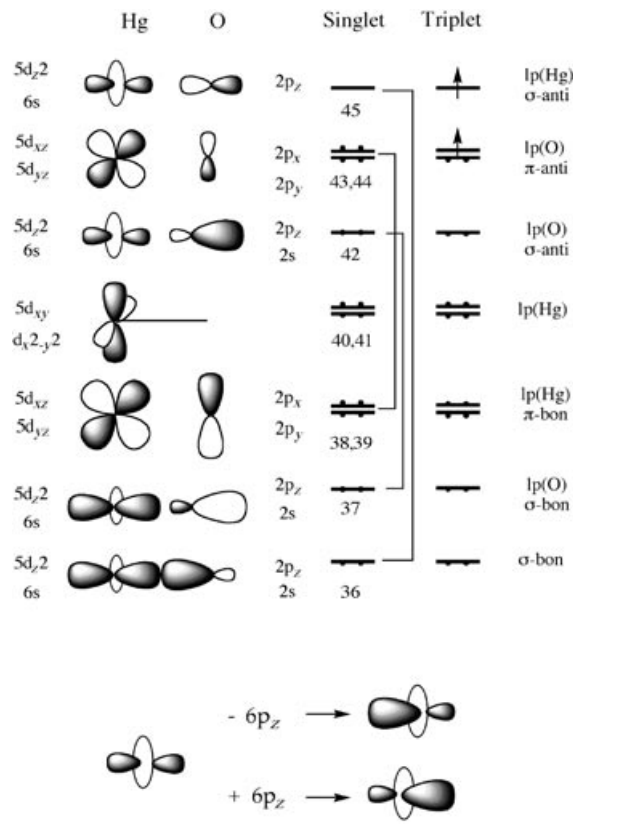

Figure 1. *Molecular orbital diagram of the nine (ten) valence orbitals of the HgO($^1\Sigma^+$) and HgO($^3\Pi$) state according to IORAmm/B3LYP/[17s14p9d5f]/aug-cc-pVTZ calculations. The atomic orbitals participating in the molecular orbitals are indicated and the nature of the molecular orbital is given [lp(Hg) or lp(O): lone pair orbital at Hg or O; σ-bon or π-bon: σ- or π-bonding orbital; σ-anti or π-anti: σ- or π-antibonding orbital]. The bonding and the corresponding antibonding molecular orbitals are connected by brackets. The mixing possibilities between the 5d$_{z^2}$ and 6p$_z$ atomic orbitals (AOs) of Hg are shown at the bottom.*

Bonding in the Monomers

Mercury possesses a closed-shell configuration ($\ldots 4f^{14}5d^{10}6s^2$) that can lead only to weak van der Waals interactions similar to the case of beryllium. The mercury dimer, Hg_2 is somewhat less stable ($D_e = 380 \pm 25$ cm^{-1}; $r_e = 3.69 \pm 0.01$ Å)[33] than Be_2 ($D_e = 790 \pm 30$ cm^{-1}).[34] Covalent bonding between E (O, S, Se) and Hg will be only possible if there is a charge transfer of approximately one electron from Hg to E as is really found in the case of singlet HgO (NBO charge: ± 0.9 electrons (e) according to IORAmm/B3LYP calculations). In this way, $Hg^+(\ldots 4f^{14}5d^{10}6\,s^1)$ and O^- ($\ldots 2s^2 2p_x^2 2p_y^2 2p_z^1$) possess one electron each and are prone to establishing a single covalent bond. Such a bond should possess a bond length of about 2.05 Å as was found for solid HgO.[5,13] The calculated HgO bond length for the gas phase is 1.875 Å (IORAmm/CCSD(T), Table 1), which is clearly shorter and may indicate a stronger bond. The calculated dissociation energy of 2.9 kcal mol^{-1} (IORAmm/CCSD(T), Table 1) however suggests sooner the existence of a van der Waals complex rather than a covalently and electrostatically bonded molecule.

The diagram of the nine valence orbitals of singlet HgO (Figure 1) reveals that due to the charge transfer a covalent bond between Hg and O is established, which involves the 6s and 5d$_{z^2}$ orbitals of the Hg atom and the 2s and 2$_{p_z}$ of the O atom [molecular orbital (MO) 36]. At the same time, there are six valence orbitals (indicated in Figure 1 by brackets) that are involved in lone pair–lone pair (lp–lp) repulsion. This should lead to a large destabilization energy. In the case of F–H and F–F the difference in the bond energies D_e (140.9 and 38.2 kcal mol^{-1}, respectively[31]) is approximately 100 kcal mol^{-1} as a result of the polarity of the F–H bond and destabilizing lp–lp interactions in the F–F bond. According to estimates, the expected D_e(F–F) value of 111 kcal mol^{-1} is lowered by more than 60 kcal mol^{-1} because of lp–lp repulsion.[31] In the case of the HgO molecule, the stabilization energy due to covalent (and electrostatic) bonding is annihilated by lp–lp repulsion almost completely so that just the small bonding energy of 2.9 kcal mol^{-1} remains. For comparison, the D_0 value of BeO, for which no lp–lp repulsion exists, is as large as 104 kcal mol^{-1}.[35]

In the triplet state, the antibonding σ orbital becomes singly occupied, which weakens covalent bonding. There are however two effects that improve the bonding energy relative to that of the singlet: 1) One of the π-type lone pair orbitals is now singly occupied (Figure 1) so that electron pair repulsion is decreased (σ bonding is exchanged against π bonding). 2) The singly occupied σ-antibonding orbital can decrease its antibonding character by mixing in the 6p$_z$(Hg) orbital thus leading to a net effect of somewhat larger covalent HgO bonding (see bottom of Figure 1). MO 45 adopts Hg σ lone pair character and the charge transfer from Hg to O is partially re-

verted. The calculated NBO charge decreases from 0.9 (singlet state) to 0.4 e (triplet state) according to IORAmm/B3LYP calculations.

Since MP2 exaggerates pair correlation effects, it predicts a much too high bonding energy for the singlet and a too low stabilization energy for the triplet, which has one electron pair less (Table 1). MP4 corrects for the exaggeration of the pair correlation effects by the inclusion of disconnected Q excitations. Also, the T excitations partially take over the description of correlation effects and, since these effects are uncoupled, correlation in the closed-shell system is again exaggerated.[36] A balanced description is only obtained by CCSD(T), which corresponds to a full configuration interaction (CI) in the SD space (no longer any exaggeration of pair correlation and orbital relaxation effects) and possesses in the T space important TT coupling effects.[37] Therefore, the IORAmm/CCSD(T) D_e(HgO) value of 2.91 kcal mol^{-1} (Table 1) is the most reliable value obtained herein.

The use of the Feenberg scaling procedure, Equations (1) and (2), ameliorates the overbinding of IORAmm/MP4 almost completely and brings the IORAmm/FE$^{(4)}_{\lambda^{(3)}}$ dissociation energies to within 1 kcal mol^{-1} of the IORAmm/CCSD(T) values. The information necessary to calculate the Feenberg correlation energies is contained in Table 2 for both monomeric and dimeric species. For the monomers, the dissociation energy D_e based on Feenberg scaling is presented in the last column of Table 1.

In the case of the triplet states, distinct three-electron correlation effects are encountered in the π orbitals (Figure 1). Therefore, IORAmm/MP4 provides a reasonable description of the triplet bonding energy, which has only to be corrected for the TT coupling effect.[37] IORAmm/CCSD(T) gives a value of 4.2 kcal mol^{-1} for HgO (Table 1). This reflects the small stabilizing effects resulting from the occupation of the MO 45 discussed above. Feenberg scaling of the IORAmm/MP4 energy has only a marginal effect on the triplet-state dissociation energy.

It is interesting to note that IORAmm/B3LYP contrary to IORAmm/MP2 and IORAmm/MP4 leads to the right state ordering in HgO and HgSe and predicts in the case of the singlet species D_e values, which are close to the IORAmm/CCSD(T) binding energies (see Table 1). The triplet HgO binding energy (9.8 kcal mol^{-1}) is exaggerated by a factor of 2 relative to the IORAmm/CCSD(T) value. The bonding in the other triplet species is also overestimated; however, this overestimation becomes less important with increasing atomic number of E.

Bonding in the Dimers

In the case of the HgO dimer, we find two isomers of comparable stability, namely the O·Hg$_2$·O isomer with the short Hg–Hg bond and the Hg·O$_2$·Hg isomer with the short O–O bond. We will discuss first bonding in the isomer with the short Hg–Hg bond.

In Figure 2, the 18 valence orbitals of the O·Hg$_2$·O isomer in its singlet state are given in an orbital scheme and some orbitals are shown explicitly, for example the 11b$_{2u}$ and 9b$_{3g}$ orbitals, which form a pair of a Hg–Hg π-bonding and a Hg–Hg π*-antibonding orbitals with a zero effect on Hg–Hg net bond-

Table 2. *Ab initio SCF and correlation energies [in hartree] for atoms and monomeric and dimeric HgE (E = O, S, Se) species. All calculations employ the IORAmm/B3LYP optimized geometry and the IORAmm quasirelativistic Hamiltonian.*

Molecule (State)	E_{SCF}	$\Delta E_{CCSD(T)}$ [a]	$E^{(2)}_{MP}$ [b]	$E^{(3)}_{MP}$	$E^{(4)}_{MP}$	$\Delta E^{(4)}_{\lambda^{(3)}}$ [c]
Hg (^{1}S)	−19591.2292627	−0.8164600	−0.8863501	+0.1230228	−0.0708273	−0.8147176
O (^{3}P)	−74.8683803	−0.1679505	−0.1482829	−0.0144939	−0.0041377	−0.1680516
S (^{3}P)	−398.6324941	−0.1845514	−0.1571712	−0.0195709	−0.0065931	−0.1857194
Se (^{3}P)	−2427.5699782	−0.2403150	−0.2230657	−0.0044915	−0.0147539	−0.2432356
HgO ($^1\Sigma^+$)	−19665.9973379	−1.0893524	−1.1510298	+0.1412064	−0.1088629	−1.0899445
HgO ($^3\Pi$)	−19666.0779047	−1.0105688	−1.0539040	+0.1086998	−0.0791278	−1.0059594
HgS ($^1\Sigma^+$)	−19989.8207351	−1.0520073	−1.0998003	+0.1146730	−0.0886504	−1.0529107
HgS ($^3\Pi$)	−19989.8594246	−1.0129986	−1.0510142	+0.1021327	−0.0791718	−1.0103564
HgSe ($^1\Sigma^+$)	−22018.7558039	−1.1029780	−1.1597899	+0.1284121	−0.0960487	−1.1038961
HgSe ($^3\Pi$)	−22018.7925812	−1.0695256	−1.1185599	+0.1186083	−0.0883603	−1.0673327
O·Hg$_2$·O (^{1}A$_g$)	−39332.0379761		−2.3237545	+0.3059035	−0.2763026	−2.2163078
O·Hg$_2$·O (^{3}B$_{2u}$)	−39332.0907796		−2.3430647	+0.2792187	−0.2795428	−2.2692574
Hg·O$_2$·Hg (^{1}A$_g$)	−39332.0141326		−2.3417391	+0.2885572	−0.2325088	−2.2238210
Hg·O$_2$·Hg (^{3}A$_u$)	−39332.1130497		−2.3473094	+0.2756617	−0.2436959	−2.2520712
S·Hg$_2$·S (^{1}A$_g$)	−39979.7300669		−2.2073875	+0.2345876	−0.1919338	−2.1186849
S·Hg$_2$·S (^{3}B$_{2u}$)	−39979.7049987		−2.3105662	+0.2543247	−0.2523426	−2.2454703
Se·Hg$_2$·Se (^{1}A$_g$)	−44037.5955286		−2.3401475	+0.2676092	−0.2117912	−2.2309365
Se·Hg$_2$·Se (^{3}B$_{2u}$)	−44037.5677226		−2.4475764	+0.2890285	(−0.1276756)[d]	
sg-Hg$_2^{2+}$·q$_2^-$ [e]	−39182.4935434		−1.6654233	+0.2171593	−0.1273140	−1.5418528
tg-Hg$_2^{2+}$·q$_2^-$ [f]	−39182.4792824		−1.6640402	+0.2114605	−0.1288479	−1.5476475
sg-Hg$^+$·q$^-$ [g]	−19591.1970558		−0.8047755	+0.1010466	−0.0541460	−0.7440753
tg-Hg$^+$·q$^-$ [h]	−19591.1952955		−0.8048074	+0.1010553	−0.0541403	−0.7440943

[a] IORAmm/CCSD(T) correlation energy. [b] $E^{(n)}_{MP}$ denotes the nth-order contribution to the IORAmm/MP correlation energy. [c] $\lambda^{(3)}$ Feenberg correlation energy obtained from the fourth-order IORAmm/MP correlation energy. [d] MP4(SDQ) contribution to the correlation energy. [e] Hg$_2^{2+}$ augmented with two negative charges (q$^-$). The geometry of the singlet ^{1}A$_g$ state of the Hg$_2$O$_2$ cluster is used. [f] Hg$_2^{2+}$ augmented with two negative charges (q$^-$). The geometry of the triplet ^{1}A$_g$ state of the Hg$_2$O$_2$ cluster is used. [g] Hg^{2+} augmented with a negative charge placed at the same distance as in sg-Hg$_2^{2+}$·q$_2^{2-}$. [h] Hg^{2+} augmented with a negative charge placed at the same position as in tg-Hg$_2^{2+}$·q$_2^{2-}$.

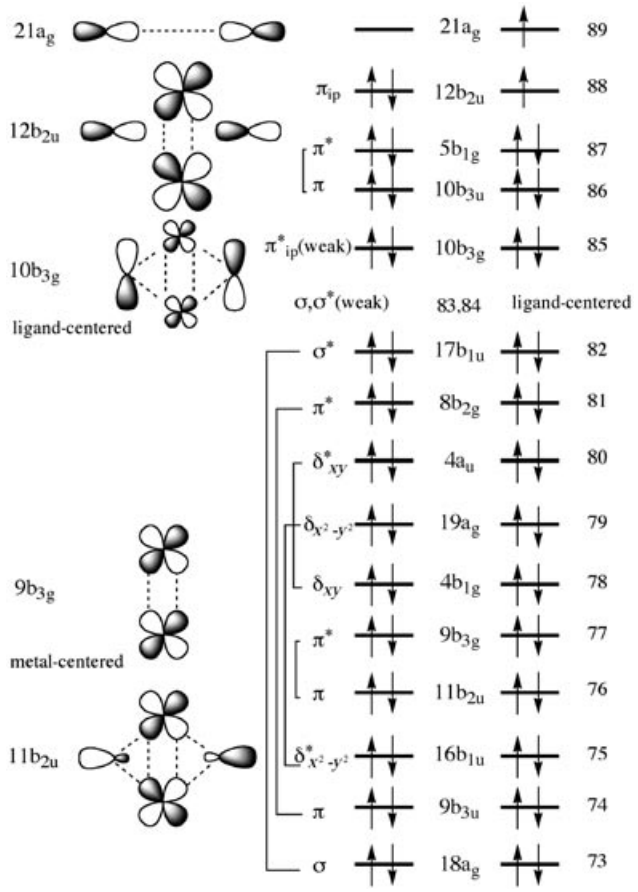

Figure 2. *Schematic representation of the 18 (19) valence molecular orbitals of the Hg_2O_2 (^1A_g) and Hg_2O_2 ($^3B_{2u}$) states according to IORAmm/B3LYP/[17s14p9d5f]/aug-cc-pVTZ calculations. Some of the orbitals are shown schematically. Bonding overlap is indicated in the MO diagrams by dashed lines. In the singlet state, bonding is established by two-electron four-center interactions (MO 11 b_{2u}) and two-electron two-center bonding (MO 12 b_{2u}). The Hg–Hg interactions have π-bond character. In the triplet state, the Hg–Hg interaction is of the three-electron nature and complemented by a single-electron through-space interaction between the O atoms.*

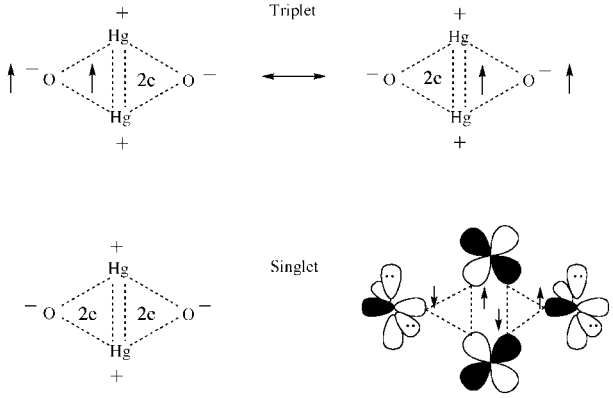

Scheme 1. *Schematic description of bonding in Hg_2O_2 (^1A_g) and Hg_2O_2 ($^3B_{2u}$). In the singlet state, two-electron three-center bonding (indicated by the dashed lines and the symbol 2e) lead to a Hg–Hg bond order of 0.66. The orbitals involved in bonding are indicated and their occupation is schematically shown. In the triplet state, two resonance structures lead to an extra stabilization.*

ing. Bonding in the ^1A_g state is established by the $12b_{2u}$ and $10b_{3g}$ MO pair (Figure 2), which leads to some net Hg–Hg bonding because of the larger magnitude of the d_{xz}-orbital coefficients in the bonding MO $12b_{2u}$. According to the calculated B3LYP NBO charges, there is a charge transfer of 1.2 electrons from each Hg atom to an O atom so that each Hg and O atom possesses about one electron (together four) for bonding. Delocalization of the four bonding electrons over four centers leads to two-electron four-center bonds or in a representation using localized orbitals, to two two-electron three-center bonds (Scheme 1). This suggests a Hg–Hg bond order of 0.66 (the actual IORAmm/B3LYP Mulliken overlap population is 0.658).

Typical Hg–Hg bond lengths in XHgHgX compounds (X = halogen) containing the Hg_2^{2+} dication with Hg(I) are in the range 2.5 to 2.6 Å.[12,13,38] In the solid state, Hg prefers to adopt the oxidation state (II) and to form –Hg–O–Hg–O– chains with OHgO angles close to 180° and HgOHg angles close to 109°.[5] In the gas phase, this is no longer possible and Hg is forced to adopt the mercury halide structure with the Hg_2^{2+} dication unit as a much more stable arrangement than the monomeric HgE arrangement. The only way of accommodating the negatively charged O atoms is to place them into a bridge position. The IORAmm/B3LYP geometry optimization of linear OHgHgO species, similar to mercury halides, lead to structures characterized by imaginary vibrational frequencies. The only true minima on the singlet and triplet potential surfaces of the HgE dimers possessing a Hg–Hg bond are the cyclic diamond core structures with the geometric parameters reported in Table 3 (for the minima with an O–O bond, see below).

The Hg–Hg distance in the dimer structures (see Table 3) depends on the electronegativity of the bridging atom E: The larger the electronegativity of E is, the larger the charge transfer from Hg to E is and the better the Hg–Hg bond can be established (Hg–Hg bond lengths for E = O: 2.773; E = S: 2.778; E = Se: 2.792 Å; Table 3). Similar trends were observed for the halides XHgHgX (Hg–Hg bond lengths for X = F: 2.51; X = Cl:

Table 3. *Bond lengths [in Å] and NBO charges [in e] of dimeric HgE (E = O, S, Se) optimized at the IORAmm/B3LYP level of theory.*

Molecule (State)	R_{Hg-Hg}	R_{E-E}	R_{Hg-E}	q_{NBO}
O·Hg_2·O (^1A_g)	2.773	3.264	2.141	±1.211
O·Hg_2·O ($^3B_{2u}$)	3.019	3.065	2.151	±0.976
Hg·O_2·Hg (^1A_g)	4.192	1.624	2.248	±0.729
Hg·O_2·Hg (^3A_u)	4.828	1.370	2.509	±0.402
S·Hg_2·S (^1A_g)	2.778	4.113	2.482	±0.915
S·Hg_2·S ($^3B_{2u}$)	3.074	3.968	2.510	±0.761
Se·Hg_2·Se (^1A_g)	2.792	4.346	2.583	±0.822
Se·Hg_2·Se ($^3B_{2u}$)	3.124	4.179	2.609	±0.636

2.53; X = Br: 2.58; X = I: 2.69 Å)[12,13] where however one has to consider that in condensed phases the mercury halides adopt a linear rather than cyclic structure. This leads in solution to an extra electrostatic stabilizing effect because the solvation energy is larger for linear rather than cyclic structures.

The triplet state possesses the $^3B_{2u}$ configuration because the b_{2u}-symmetrical HOMO and the a_g-symmetrical LUMO of the singlet state are now singly occupied (Figure 2).

This leads to a decrease in Hg–Hg bonding, however to an increase in Hg–O bonding, which, because of the factor 4, outweighs the weakening of the Hg–Hg bond. The calculated Hg–Hg bond lengths of 3.019 (E = O), 3.074 (E = S), and 3.124 Å (E = Se, Table 2) are somewhat longer than in the Hg_2^{2+} dication. Hence, the $^3B_{2u}$ state of the O·Hg_2·O isomer does not gain by increased Hg–Hg bonding, but by a reduction of Hg–O antibonding. The optimized Hg–O distance in the triplet cluster is only marginally longer than in the singlet species (2.151 Å versus 2.141 Å). Considering a substantial lengthening of the Hg–Hg bond (by 0.246 Å from 2.773 to 3.019 Å, Table 3) the Hg–O bond length of 2.223 Å should have resulted if the oxygen anions remained in the same positions as in the singlet species. The actual Hg–O bond (2.151 Å) is shorter than this estimate which suggests the Hg–O bond strengthening in the triplet state.

One of the unpaired electrons can form a one-electron three-center bond (see Scheme 1) whereas the second electron can only contribute to a long-range dispersion attraction between the E atoms at 3.065 (E = O), 3.968 (E = S), and 4.179 Å (E = Se). There are two important resonance structures (see Scheme 1), which reestablish D_{2h} symmetry for the triplet dimer. A jumping of the unpaired electron engaged in Hg–Hg bonding from one three-membered ring to the other requires the reverse jumping of the electron pair in the lower $11b_{2u}$ MO. The electron leaps are accompanied with a change of the orbitals especially at the O atoms, which are more contracted in the electron pair situation. The three-electron correlation effects add to the stability of the triplet, its adequate description requires however a method accounting for connected T excitations. Clearly, MP2, MP3, and MP4(SDQ) cannot provide these correlation effects and, therefore, underestimate the stability of the $^3B_{2u}$ state severely (Table 4).

Full MP4 includes T excitations and accounts therefore for three-electron correlation effects.[36] Accordingly, IORAmm/MP4 predicts the triplet O·Hg_2·O isomer approximately 50 kcal mol^{-1} more stable than IORAmm/MP2 or IORAmm/MP4(SDQ) do (see Table 4). Similarly dramatic increases in the stability are also found for the $^3B_{2u}$ state of S·Hg_2·S and Se·Hg_2·Se (see Table 4). Previous investigations showed[36,37] that MP4 exaggerates the three-electron correlation effects. Feenberg scaling improves considerably[24] the convergence of the MP series and leads to lower stability of the triplet states than predicted by IORAmm/MP4, which however is still larger than that predicted by IORAmm/MP2 or IORAmm/MP4(SDQ). We conclude that the values obtained by the Feenberg scaling procedure are more reliable than any value obtained by the other wave function methods reported in Table 4.

Considering the fact that B3LYP leads to reasonable values for the monomers and approaches for the singlet states even the accuracy of the CCSD(T) calculations, its failure in the case of the dimers is dramatic (see Table 4). However, the mercury chalcogenide dimers are species for which higher-order correlation effects play an important role. At the Hartree–Fock level, the atomization energies for both states are negative. The correlation corrections of the atomization energies introduced by MP2 are about 160 and 170 kcal mol^{-1}, respectively; those introduced by the T excitations at MP4 are 55 and 52 kcal mol^{-1}, respectively (Table 4). Thus, it is not surprising that the stability of the triplet states is severely underestimated by a functional such as B3LYP, which admixes some Hartree–Fock exchange to DFT exchange. For instance, a BPW91[39] calculation of the O·Hg_2·O isomer yields the atomization energy of 68.0 kcal mol^{-1} for the singlet and of 68.3 kcal mol^{-1} for the triplet state. Switching to local density approximation (LDA)[40] increases the stability of the dimer of mercury oxide even further, namely to 131.8 kcal mol^{-1} for the singlet and 126.7 kcal mol^{-1} for the triplet state. These results show that both dynamic and nondynamic electron correlation effects, which are included into the DFT calculations either explicitly via the correlation functional or implicitly via the local (or semilocal) exchange functional and its self-interaction error,[41] are underestimated by a hybrid functional such as B3LYP in two ways: 1) The admixture of 20% exact exchange leads to a smaller self-interaction error (SIE) and, by this, to a significant reduction of nondynamic electron correlation.[41] 2) The LYP correlation functional was derived from the Colle–Salvetti description of the He atom[42] and as such it is not suited for describing pronounced three- or even higher-electron correlation effects. Contrary to the case of the monomer states, the dimer states are characterized by electrostatic interactions (as a result of charge transfer) connected with distinct high-order correlation effects, no longer tractable

Table 4. *Electronic atomization energies [in kcal mol^{-1}] of dimeric HgE (E = O, S, Se) species calculated at the IORAmm/B3LYP geometry. All calculations employ the IORAmm quasirelativistic Hamiltonian.*

Molecule (State)	B3LYP	MP2	MP4(SDQ)	MP4(full)	$FE^{(4)}_{\lambda^{(3)}}$ [a]
O·Hg2·O (^1A_g)	40.01	60.98	39.36	84.53	58.65
O·Hg2·O ($^3B_{2u}$)	46.98	106.23	96.04	148.56	125.01
Hg·O2·Hg (^1A_g)	37.80	57.24	20.99	64.20	48.40
Hg·O2·Hg (^3A_u)	66.48	122.87	107.83	144.94	128.20
S·Hg2·S (^1A_g)	69.20	79.63	63.96	85.53	78.04
S·Hg2·S ($^3B_{2u}$)	45.35	128.64	111.94	160.07	141.87
Se·Hg2·Se (^1A_g)	59.06	74.24	60.38	80.60	70.33
Se·Hg2·Se ($^3B_{2u}$)	35.94	124.24	108.31		(138.24)[b]

[a] $\lambda^{(3)}$ Feenberg extrapolation energy obtained from the fourth-order IORAmm/MP energy. [b] Value obtained from extrapolation using the energies for S·Hg_2·S($^3B_{2u}$).

by B3LYP (or hybrid functionals, in general, due to the admixture of the HF exchange). The relative stability of the singlet state (with respect to the triplet) is overestimated by approximate density functionals because of the larger SIE. The SIE for the triplet state (described within the spin-unrestricted DFT formalism) is considerably smaller than that for the singlet state.[43] Since the triplet state is more stable than the singlet state, this results in an artificial narrowing of the singlet–triplet gap for the dimers as predicted by DFT because of an overstabilization of the singlet.

The second isomer, $Hg{\cdot}O_2{\cdot}Hg$, is of comparable stability with the first one. Its ^3A_u ground state is 3.2 kcal mol^{-1} (Feenberg atomization energy: 128.2 kcal mol^{-1}, Table 4) more stable than that of the $O{\cdot}Hg_2{\cdot}O$ isomer whereas its ^1A_g excited state is 10 kcal mol^{-1} (Feenberg atomization energy: 48.4 kcal mol^{-1}) less stable than the corresponding $O{\cdot}Hg_2{\cdot}O$ state. The change in bonding is reflected by the fact that O–O bonding orbital $21a_g$, which is singly occupied in the $^3B_{2u}$ state or empty in the ^1A_g state of the $O{\cdot}Hg_2{\cdot}O$ isomer (Figure 2), is doubly occupied in the $Hg{\cdot}O_2{\cdot}Hg$ isomer. The MO $12b_{2u}$ becomes empty for the latter isomer so that its bonding Hg–Hg and antibonding O–O interactions are no longer relevant. Frontier orbitals are now MO $5b_{1g}$ (HOMO in the singlet or SOMO in the triplet state of the $Hg{\cdot}O_2{\cdot}Hg$ isomer) and MO $19b_{1u}$, (not shown in Figure 2; LUMO in the singlet and the second SOMO in the triplet state), where the latter corresponds to the O–O antibonding π MO. The new orbital occupation characterizes the forming of a short O–O bond and the cleavage of the Hg–Hg bond.

The charge transfer from Hg to the O–O unit is smaller for the $Hg{\cdot}O_2{\cdot}Hg$ isomer (singlet: 0.729 e, triplet: 0.402 e; Table 3) than for the $O{\cdot}Hg_2{\cdot}O$ isomer (singlet: 1.211 e; triplet: 0.976 e) where again the triplet state has the lower ionic character. The smaller charge transfer is due to the fact that negative charges at the O–O unit reduce O–O bonding and by this the stability of the $Hg{\cdot}O_2{\cdot}Hg$ isomer, which will be not the case if the two O atoms are not bonded as in the first isomer.

We also checked the possibility that the HgO dimer forms a four-membered ring or a tetrahedron, however in both cases the $O{\cdot}Hg_2{\cdot}O$ or the $Hg{\cdot}O_2{\cdot}Hg$ were obtained. Hence, these structures can only function as transition states between the two isomers, which will be investigated in a forthcoming paper focusing on the question of bond stretch isomerism for the HgO dimers.[44]

Concluding this section, the results of the high-level ab initio calculations indicate that the monomeric HgE (E = O, S, Se) species have dissociation energies which vary between 2 and 6 kcal mol^{-1} (see Table 1). These calculations do not include spin–orbit (SO) coupling, however the energetic effect of the SO interaction is expected to be minimal (see also ref. [9]). Indeed, the unpaired electrons in the triplet states of the mercury chalcogenides are located predominantly in the 6s orbital of the Hg atom and the $2p_{x(y)}$ orbitals of the O atom, which implies weak first-order SO interaction. In the dimeric species, the unpaired electrons are located almost exclusively at the oxygen atoms, which also does not suggest a substantial energy shift caused by the SO interactions. Thus, the calculated atomization energies of the dimers, which for the triplet states of $(HgE)_2$ are as large as 125 kcal mol^{-1} (E = O), 142 kcal mol^{-1} (E = S), and 138 kcal mol^{-1} (E = Se), respectively, should be sufficiently reliable to be compared with the corresponding experimental data. Noteworthy is that there are two HgO dimers differing only by 3.2 kcal mol^{-1} in their triplet states. The chemical consequences of this finding have to be discussed in the following.

4. Chemical Relevance of the Results

Accurate ab initio electronic structure methods were used to determine the atomization energy of monomeric HgE and dimeric $(HgE)_2$ (E = O, S, Se). In agreement with the previous theoretical study of gaseous mercury oxide,[9] IORAmm/CCSD(T) predicts the dissociation energy of HgO to be just 4 kcal mol^{-1} confirming that the compound experimentally found to possess a dissociation energy D_0 of 53 ± 8 kcal mol^{-1}[7] was definitely not HgO. The atomization energies of the mercury monoxide dimers $O{\cdot}Hg_2{\cdot}O$ and $Hg{\cdot}O_2{\cdot}Hg$ are calculated to be 125 and 128 kcal mol^{-1}, respectively, which, when corrected for zero-point vibrational energies and thermal energies (ca. 5.8 and 6.5 kcal mol^{-1} according to IORAmm/B3LYP calculations), yields an atomization energy per monomer of 59.6 to 60.8 kcal mol^{-1} in a reasonable agreement with the experimental value of 53 ± 8 kcal mol^{-1}.

This finding suggests that under the conditions of the mass spectrometric experiment the mercury oxide dimer rather than the monomer is present in the gas phase. Consequently, the reaction given in Equation (3) (see Equation (15) in ref. [7]) used to determine the D_0 value of the assumed monomer:

$$HgO(g) \rightarrow \frac{1}{3}\langle HgO\rangle + \frac{2}{3}Hg(g) + \frac{1}{3}O2(g) \quad \langle\rangle: \text{ solid phase} \qquad (3)$$

has to be corrected for the dimer $(HgO)_2$ according to Equation (4)

$$(HgO)_2(g) \rightarrow \frac{1}{3}\langle HgO\rangle + \frac{4}{3}Hg(g) + \frac{2}{3}O_2(g) \qquad (4)$$

and the results of the determination of D_0 should be reassessed. There is a large dimerization energy of 120.7 kcal mol^{-1} for two HgO monomers in their triplet state. This, however, does not imply that the formation of the dimers proceeds via the monomers. In the vaporization process of solid mercury oxide, the –Hg–O–Hg–O– chains are fragmented and both Hg and O atoms as well as fragments such as HgO, OHgO or HgOHgO can be formed where in the latter case either singlet or triplet states are adopted. Since molecular oxygen is withdrawn from the gaseous mixture[7] it is likely that one of the four reactions [see Equations (5)–(8)] takes place:

$$HgO^{1,3} + HgO^{1,3} \rightarrow (HgO)_2^{1,3} \qquad (5)$$

$$Hg^{1,3} + OHgO^{1,3} \rightarrow (HgO)_2^{1,3} \qquad (6)$$

$$O^3 + HgOHg^3 \rightarrow (HgO)_2^{1,3} \qquad (7)$$

$$OHgOHg^{1,3} \rightarrow (HgO)_2^{1,3} \qquad (8)$$

Depending on the vapor pressure one reaction will be more likely than the others. In any case, reaction (8) requires the least geometrical and electronic rearrangement because the two O or the two Hg atoms have only to establish a bonding interaction and the terminal Hg (O) atom has to flip into a bridging position. Clearly, these considerations suggest that there should not be any preference for the singlet or the triplet dimer and, even if the concentration of the monomer is rather small, a mixture of monomer and dimer will be more likely than an absolute dominance of any of the $(HgO)_2$ dimers. This is probably the reason for the large experimental error bars of ± 8 kcal mol^{-1}. Therefore, the calculated D_0 value of 59–60 kcal mol^{-1} for the dimer may be more trustful than the experimental value. Nevertheless, there is an agreement between the measured value of 53 ± 8 kcal mol^{-1}[7] and the calculated value of 59 kcal mol^{-1}, which suggests that most of the dimer is in the triplet state.

From this study it becomes also clear that the values of 53 ± 8 kcal mol^{-1}[7] or 59 kcal mol^{-1} are by no means HgO dissociation energies. In the O·Hg_2·O isomer there are four HgO and one Hg–Hg bonding interactions according to the electronic structure analysis carried out herein. We calculate the Hg–Hg dissociation energy in the Hg_2^{2+} dications to be -61.04 kcal mol^{-1} (Feenberg energies), which of course reflects the Coulomb repulsion energy of two positive charges. If this is considered, *a* D_e value of 68.37 kcal mol^{-1} results, which is comparable with the Au–Au dissociation energy $D_0 = 53.8 \pm 0.5$ kcal mol^{-1}.[31] In the mercury oxide dimer, the repulsion between positive charges at the Hg atoms is largely compensated by charge attraction between Hg and O atoms, that is, the bonding in the dimeric clusters is predominantly electrostatic in nature. For the purpose of estimating the magnitude of the electrostatic component of Hg–O bonding, we carried out calculations for a model dimer, in which the oxygen atoms of the O·Hg_2·O isomer are replaced by negative unit charges q^- retaining the geometry of the dimer. In this way, a mercury dimer dication with stretched Hg–Hg bond and two counterions in the bridge positions results.

The calculations of the $Hg_2^{2+}\cdot q_2^-$ cluster in its singlet state were carried out at the geometry of both the singlet ^1A_g [labeled as singlet geometry (sg) $Hg_2^{2+}\cdot q_2^-$) and triplet $^3B_{2u}$ state [labeled as triplet geometry (tg) $Hg_2^{2+}\cdot q_2^-$) of the Hg_2O_2 cluster. Calculated energies are reported in Table 2 and compared with the energies of fragments $Hg^+\cdot q^-$ in which the negative charge was placed at the same position as in the sg-$Hg_2^{2+}\cdot q_2^-$ and in the tg-$Hg_2^{2+}\cdot q_2^-$ clusters. The resulting association energies obtained from Feenberg scaling are 96.92 kcal mol^{-1} for the singlet geometry and 92.96 kcal mol^{-1} for the triplet geometry. These energies have to be compared with the true association energies of the singlet (50.03 kcal mol^{-1}) and triplet (116.39 kcal mol^{-1}) state of the Hg_2O_2 cluster calculated relative to the binding energy of the monomer (4.31 and 2.17 kcal mol^{-1}, see Table 1). The comparison reveals that, in view of charge-transfer values unequal ± 1 used in the electrostatic model (compare with Table 3), the triplet state of the Hg_2O_2 cluster is (electrostatically) stabilized by approximately 5.9 kcal mol^{-1} per Hg–O bond whereas the singlet state is destabilized by almost 11.5 kcal mol^{-1} per bond. This leaves for the covalent corrections of the four HgO interactions just somewhat more than 2 kcal mol^{-1}. This is consistent with the dissociation energies found for the monomer (Table 1) and the qualitative discussion based on the molecular orbital diagram in Figure 2.

We conclude that covalent bonding between Hg and O is rather weak (see Scheme 2). This is due to strong lp–lp repulsion, which decreases covalent bonding to just a couple of kcal mol^{-1}. Since covalent bonding is only possible as a result of a charge transfer from Hg to O (Scheme 2), it is supported by electrostatic bonding. This becomes especially obvious for the dimer. The large atomization energies of the dimer are basically a result of electrostatic interactions between charged atoms, that is, a Hg_2^{2+} dication is internally *solvated* by two negative charges associated with the O atoms. The HgO dissociation energy D_0 is misleading in several ways: 1) It belongs to the dimer rather than the monomer. 2) It results from four Hg–O electrostatic interactions with only some weak covalent bonding. 3) It belongs to a triplet rather than a singlet ground state.

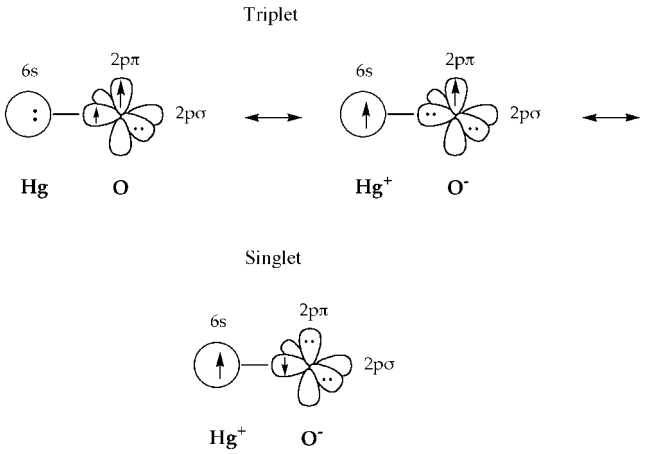

Scheme 2. *Schematic description of bonding in HgO($^1\Sigma^+$) and HgO($^3\Pi$). A charge transfer of one electron from Hg to O is assumed; this leads to a single covalent HgO bond in the singlet state. In the triplet state, a three-electron bond is established involving either the two 6s electrons of the Hg atom or, in the case of a charge transfer, two 2pσ electrons of the O atom. In any case, one of the O lone-pair orbitals is singly occupied thus reducing lone pair–lone pair repulsion and stabilizing the triplet state relative to the singlet state.*

The bonding is different in the dimer compared to that in the monomer. In Figures 1 and 2, each bonding MO (HgO in Figure 1, HgHg in Figure 2) is connected with its antibonding MO by a bracket. In this way, it becomes directly obvious that HgO bonding in the singlet monomer is established by the σ orbital 36 (Figure 1) and its stabilization energy is largely reduced by lp–lp repulsion. The dimer has a partial Hg–Hg bond, which is not of σ but of π character because σ bonding caused by orbital 73 is annihilated by σ antibonding caused by orbital 82 (Figure 2). The same holds for π and δ bonds of the Hg–Hg unit (Figure 2) so that just the bonding influence of the in-plane π orbital 88 remains, however reduced by the weakly antibonding π* orbital 85 (Figure 2) in line with a calcu-

lated Hg–Hg NBO bond order of 0.66. Hence, the Hg–Hg bond in the dimer is peculiar since bonding is established by a partial π bond without any supporting σ bonding.

The HgO interactions in the dimer determine the actual stability of the molecule and are also responsible for the large stability of the triplet. Orbitals 75, 76, 83, 84 lead to Hg–O bonding, which is reduced by the HgO-antibonding character of orbitals 85 and 88. As indicated in Scheme 1, four electrons remain to establish covalent bonding in the two formal three-membered rings of the dimer. If the strongly antibonding MO 88 is depopulated by one electron in the triplet state, HgO bonding will be strongly improved leading to an overall stabilization of the dimer.

Although, we have carried out rather accurate calculations, they cannot guarantee that the $Hg{\cdot}O_2{\cdot}Hg$ isomer is really more stable than the $O{\cdot}Hg_2{\cdot}O$ isomer. Reoptimization at IORAmm/CCSD(T) level could easily lead to a change in the geometry and thereby also in the relative energies of the two isomers. However, these calculations are presently not feasible. Clearly the $O–O^{2-}$ unit can establish a much stronger bond than the $Hg–Hg^{2+}$ unit. When one defines, similarly as done in the case of the Hg–Hg bond strength, the E–E bond strength BS in the E_2^{2-} dianion as the difference between the purely electrostatic repulsion of two negative charges and the quantum mechanically calculated bond dissociation energy of E_2^{2-} with respect to two E^- anions, that is, $BS = 1/r_e - [E(E_2^{2-}) - 2E(E^-)]$, where r_e is the equilibrium bond length in E_2^{2-}, then MP4 calculations predict for O_2^{2-} BS = 136.1 kcal mol^{-1} (r_e = 1.563 Å). Contrary to the $O{\cdot}Hg_2{\cdot}O$ isomer, electrostatic "solvation", electrostatic corrections considering the real charge transfer, and covalent corrections (again of about 2 kcal mol^{-1} per HgO interaction) cancel each other out to a large degree so that the O_2^{2-} bond strength contributes the major part to the stability of the $Hg{\cdot}O_2{\cdot}Hg$ isomer and is only corrected by -8 kcal mol^{-1} to obtain the atomization energy of 128.2 kcal mol^{-1}.

Assuming the same situation for the $Hg{\cdot}S_2{\cdot}Hg$ isomer, which possesses a S_2^{2-} BS of 112.8 kcal mol^{-1} (r_e = 2.168 Å), one can predict that this isomer is much less stabilized than its $S{\cdot}Hg_2{\cdot}S$ isomer. The same is true for the Se compound and therefore one can conclude that for E = S or Se only the $E{\cdot}Hg_2{\cdot}E$ isomer has to be considered although the $Hg{\cdot}E_2{\cdot}Hg$ isomer may also exist.

Chalcogenides of Group-12 Metals

The situation described for the mercury oxides holds also for the other mercury chalcogenides and, therefore, similar conclusions can be drawn in these cases. Both mercury sulfide HgS and mercury selenide HgSe are weakly bound species with the dissociation energies of just 6 and 4 kcal mol^{-1}, respectively (IORAmm/CCSD(T) results, Table 1). Dimerization leads to very stable molecules with atomization energies of 142 and 138 kcal mol^{-1} (Feenberg scaled MP4 results, Table 4). Obviously, the gas-phase chemistry of the higher mercury chalcogenides is complicated and more than one type of species is present in the gas phase.

Upon vaporization of solid mercury sulfide or solid mercury selenide, S_n and Se_n compounds with $n > 2$ can be formed. HgS possesses a larger stability in the singlet state (7.2 kcal mol^{-1}, Table 1) than the corresponding HgO monomer. Accordingly, there will be more monomer in the gas phase. Reactions with S_3, S_4, etc. fragments will be possible and it cannot be excluded that both singlet and triplet state of monomer and dimer are present in the gas phase. We note that the average of the four atomization energies is 58 kcal mol^{-1} close to the experimental value of 52 ± 5 kcal mol^{-1} (see Table 5). The low experimental value in the case of mercury selenide seems to indicate that the monomer dominates the mixture of monomeric and dimeric mercury selenides in the gas phase. It can also not be excluded that $(HgSe)_3$ with a cyclic Hg kernel plays a role and that this compound contributes to the measured D_0 value.

In Table 5, a number of measured dissociation energies of diatomic molecules containing either Hg, Zn or Cd are compared. With the exception of the obviously erroneous values of the mercury chalcogenides, there is not a single D_0 value of a diatomic molecule containing Hg, which is larger than 10 kcal mol^{-1}. It is obvious that the D_0 values of ZnE and CdE have been interpreted under the same misconception that a monomer rather than a dimer (trimer, etc.) was measured. The best theoretical values for the dissociation energy of ZnO, D_0 = 30.0 kcal mol^{-1}, and ZnS, D_0 = 24.4 kcal mol^{-1}, obtained by Boldyrev et al.[45] from QCISD/6311++G(d,p) calculations are in a substantial disagreement with the figures of 67 ± 4 (ZnO) and 54 ± 8 kcal mol^{-1} (ZnS) obtained in the mass spectrometric experiments.[7] Alternative values of $\pm 64.7 \pm 10$ and 49 ± 3 kcal

Table 5. *Comparison of some experimental bond dissociation energies D_0 of diatomic molecules HgX, ZnX, and CdX.*[a]

Molecule	D_0(Hg–X)	Molecule	D_0(Zn–X)	Molecule	D_0(Cd–X)
HgO	2.2[b]	ZnO*	$< 64.7 \pm 10$	CdO*	56.3 ± 20.0
HgS	4.8[b]	ZnS*	49.0 ± 3	CdS*	49.8 ± 5.0
HgSe	1.7[b]	ZnSe*	40.8 ± 6.2	CdSe*	30.5 ± 6.0
HgTe		ZnTe*	28.1 ± 9.3	CdTe*	23.9 ± 3.6
HgH	9.5	ZnH	20.5 ± 0.5	CdH	16.5 ± 0.1
HgI	8.3	ZnI	33 ± 7	CdI	33 ± 5
HgHg	2 ± 0.5			CdCd	1.8
HgLi	3.3			CdCl	49.8
HgNa	2.2			CdF	73 ± 5
HgHe	1.6				

[a] Dissociation energies in kcal mol^{-1} from ref. [31]. [b] Obtained in this work for the triplet ground state of the monomer.

mol^{-1}, respectively, have been published elsewhere (see Table 5).[31] Hence, there is considerable need to reinvestigate the dissociation energies of Zn and Cd chalcogenides (starred molecules in Table 5) and to consider also the reliability of Zn and Cd dissociation energies in general.[43]

Acknowledgments

A generous allotment of computer time at the National Supercomputer Center (NSC) in Linköping is gratefully acknowledged.

Keywords: ab initio calculations · gas-phase reactions · isomers · mercury

[1] H. Boudries, J. W. Bottenheim, *Geophys. Res. Lett.* **2000**, *27*, 517.
[2] J. Y. Lu, W. H. Schröder, L. A. Barrie, A. Steffen, H. E. Welch, K. Martin, L. Lockhart, R. V. Hunt, G. Boila, A. Richter, *Geophys. Res. Lett.* **2001**, *28*, 3219.
[3] R. Ebinghaus, H. H. Kock, C. Temme, J. W. Einax, A. G. Lowe, A. Richter, J. P. Burrows, W. H. Schröder, *Environ. Sci. Technol.* **2002**, *36*, 1238.
[4] C. Temme, R. Ebinghaus, J. W. Einax, W. H. Schröder, *Environ. Sci. Technol.* **2003**, *37*, 3241.
[5] L. Gmelin, *Gmelins Handbuch der anorganischen Chemie. System-Nr. 34. Quecksilber*, Springer, Berlin, **1968**.
[6] R. Butler, S. Katz, A. Snelson, J. B. Stephens, *J. Phys. Chem.* **1979**, *83*, 2578.
[7] M. Grade, W. Hirschwald, *Ber. Bunsen-Ges.* **1982**, *86*, 899.
[8] D. M. Wilmouth, T. F. Hanisco, N. M. Donahue, J. G. Anderson, *J. Phys. Chem. A* **1999**, *103*, 8935.
[9] B. C. Shepler, K. A. Peterson, *J. Phys. Chem. A* **2003**, *107*, 1783.
[10] N. B. Balabanov, K. A. Peterson, *J. Phys. Chem. A* **2003**, *107*, 7465.
[11] a) R. J. Bartlett, *J. Phys. Chem.* **1989**, *93*, 1697; b) C. J. Barden, H. F. Schaefer III, *Pure Appl. Chem.* **2000**, *72*, 1406.
[12] K. Brodersen, H.-U. Himmel in *Comprehensive Coordination Chemistry, Vol.* 5 (Ed.: G. Wilkinson), Pergamon, Oxford, **1987**.
[13] a) F. A. Cotton, G. Wilkinson, *Advanced Inorganic Chemistry,* 5th ed., Wiley, New York **1988**; b) W. W. Porterfield, *Inorganic Chemistry, A Unified Approach*, Academic Press, New York, **1993**.
[14] D. Cremer in *The Chemistry of Functional Groups, Peroxides* (Ed.: S. Patai), Wiley, New York, **1983**, p. 1 – 84.
[15] M.-M. Rohmer, M. Bernard, *Chem. Soc. Rev.* **2001**, *30*, 340.
[16] a) S. Alvarez, A. A. Palacios, G. Aullon, *Coord. Chem. Rev.* **1999**, *185–186*, 431; b) A. A. Palacios, G. Aullon, P. Alemany, S. Alvarez, *Inorg. Chem.* **2000**, *39*, 3166; c) C. Mealli, D. M. Proserpio, *J. Am. Chem. Soc.* **1990**, *112*, 5484.
[17] C. Moller and M. S. Plesset, *Phys. Rev.* **1934**, *46*, 618; for a recent review, see D. Cremer in *Encyclopedia of Computational Chemistry, Vol.* 3 (Eds.: P. v. R. Schleyer, N. L. Allinger, T. Clark, J. Gasteiger, P. A. Kollman, H. F. Schaefer III, P. R. Schreiner), Wiley, Chichester, **1998**, p. 1706.
[18] For recent reviews, see a) J. Gauss in *Encyclopedia of Computational Chemistry, Vol.* 1 (Eds.: P. v. R. Schleyer, N. L. Allinger, T. Clark, J. Gasteiger, P. A. Kollman, H. F. Schaefer III, P. R. Schreiner), Wiley, Chichester, UK, **1998**, p. 615; b) T. D. Crawford, H. F. Schaefer III in *Reviews in Computational Chemistry, Vol.* 14 (Eds.: K. B. Lipkowitz, D. B. Boyd), VCH, Weinheim, **2000**, p. 33.
[19] a) G. D. Purvis III and R. J. Bartlett, *J. Chem. Phys.* **1982**, *76*, 1910; b) K. Raghavachari, G. W. Trucks, J. A. Pople, M. Head-Gordon, *Chem. Phys. Lett.* **1989**, *157*, 479.
[20] a) A. D. Becke, *J. Chem. Phys.* **1993**, *98*, 5648; b) P. J. Stevens, F. J. Devlin, C. F. Chabalowski, M. J. Frisch, *J. Phys. Chem.* **1994**, *98*, 11623.
[21] a) A. D. Becke, *Phys. Rev. A* **1988**, *38*, 3098; b) C. Lee, W. Yang, R. G. Parr, *Phys. Rev. B* **1988**, *37*, 785.
[22] a) J. E. Carpenter, F. Weinhold, *J. Mol. Struct. (Theochem)* **1988**, *46*, 41; b) A. E. Reed, R. B. Weinstock, F. Weinhold, *J. Chem. Phys.* **1985**, *83*, 735; c) A. E. Reed, L. A. Curtiss, F. Weinhold, *Chem. Rev.* **1988**, *88*, 899.
[23] D. Cremer, Z. He, *J. Phys. Chem.* **1996**, *100*, 6173.
[24] a) Z. He, D. Cremer, *Int. J. Quantum Chem.* **1996**, *59*, 71; b) B. Forsberg, Z He, Y. He, D. Cremer, *Int. J. Quant. Chem.* **2000**, *76*, 306.
[25] C. Schmidt, M. Warken, N. C. Handy, *Chem. Phys. Lett.* **1993**, *211*, *272.*
[26] a) P. Goldhammer, E. Feenberg, *Phys. Rev.* **1956**, *101*, 1233; b) E. Feenberg, *Phys. Rev.* **1956**, *103*, 1116.
[27] O. Gropen, *J. Comput. Chem.* **1987**, *8*, 982.
[28] T. H. Dunning, Jr., *J. Chem. Phys.* **1989**, *90*, 1007.
[29] M. Filatov, *Chem. Phys. Lett.* **2002**, *365*, *222*.
[30] M. Filatov, D. Cremer, *J. Chem. Phys.* **2003**, *118*, 6741.
[31] *CRC Handbook of Chemistry and Physics on CD-ROM, 2000 Version* (Ed.: D. R. Lide), CRC Press LLC, **2000**.
[32] E. Kraka, J. Gräfenstein, M. Filatov, J. Gauss, V. Polo, A. Wu, F. Reichel, L. Olsson, Z. Konkoli, Z. He, D. Cremer, *COLOGNE 2003*, Göteborg University, Göteborg, **2003**.
[33] J. Koperski, J. B. Atkinson, L. Krause, *Chem. Phys. Lett.* **1994**, *219*, 163; J. Koperski, J. B. Atkinson, L. Krause, *Can. J. Phys.* **1994**, *72*, 1070; J. Koperski, J. B. Atkinson, L. Krause, *J. Mol. Spectrosc.* **1997**, *184*, 300.
[34] V. E. Bondybey, *Chem. Phys. Lett.* **1984**, *109*, 436.
[35] R. T. Sanderson, *Chemical Bonds and Bond Energy*, Academic Press, New York, **1976**.
[36] Y. He, D. Cremer, *Theor. Chem. Acc.* **2000**, *105*, 110.
[37] a) Z. He, D. Cremer, *Theor. Chim. Acta* **1993**, *85*, 305; b) Y. He, Z. He, D. Cremer, *Theor. Chem. Acc.* **2000**, *105*, 182.
[38] M. Kaupp, H. G. von Schnering, *Inorg. Chem.* **1994**, *33*, 4179.
[39] J. P. Perdew, Y. Wang, *Phys. Rev. B* **1992**, *45*, 13244.
[40] J. C. Slater, *Phys. Rev.* **1951**, *81*, 385; S. H. Vosko, L. Wilk, M. Nusair, *Can. J. Phys.* **1980**, *58*, 1200.
[41] a) V. Polo, E. Kraka, D. Cremer, *Mol. Phys.* **2002**, *100*, 1771; b) V. Polo, E. Kraka, D. Cremer, *Theor. Chem. Acc.* **2002**, *107*, 291; c) V. Polo, J. Gräfenstein, E. Kraka, D. Cremer, *Chem. Phys. Lett.* **2002**, *352*, 469; d) V. Polo, J. Gräfenstein, E. Kraka, D. Cremer, *Theor. Chem. Acc.* **2003**, *109*, 22.
[42] R. Colle, O. Salvetti, *Theor. Chim. Acta* **1975**, *37*, 329.
[43] D. Cremer, M. Filatov, V. Polo, E. Kraka, S. Shaik, *Int. J. Mol. Sci.* **2002**, *3*, 604.
[44] M. Filatov, D. Cremer, unpublished results.
[45] A. I. Boldyrev, J. Simons, *Mol. Phys.* **1997**, *92*, 365.

Received: December 15, 2003
Revised: July 12, 2004

